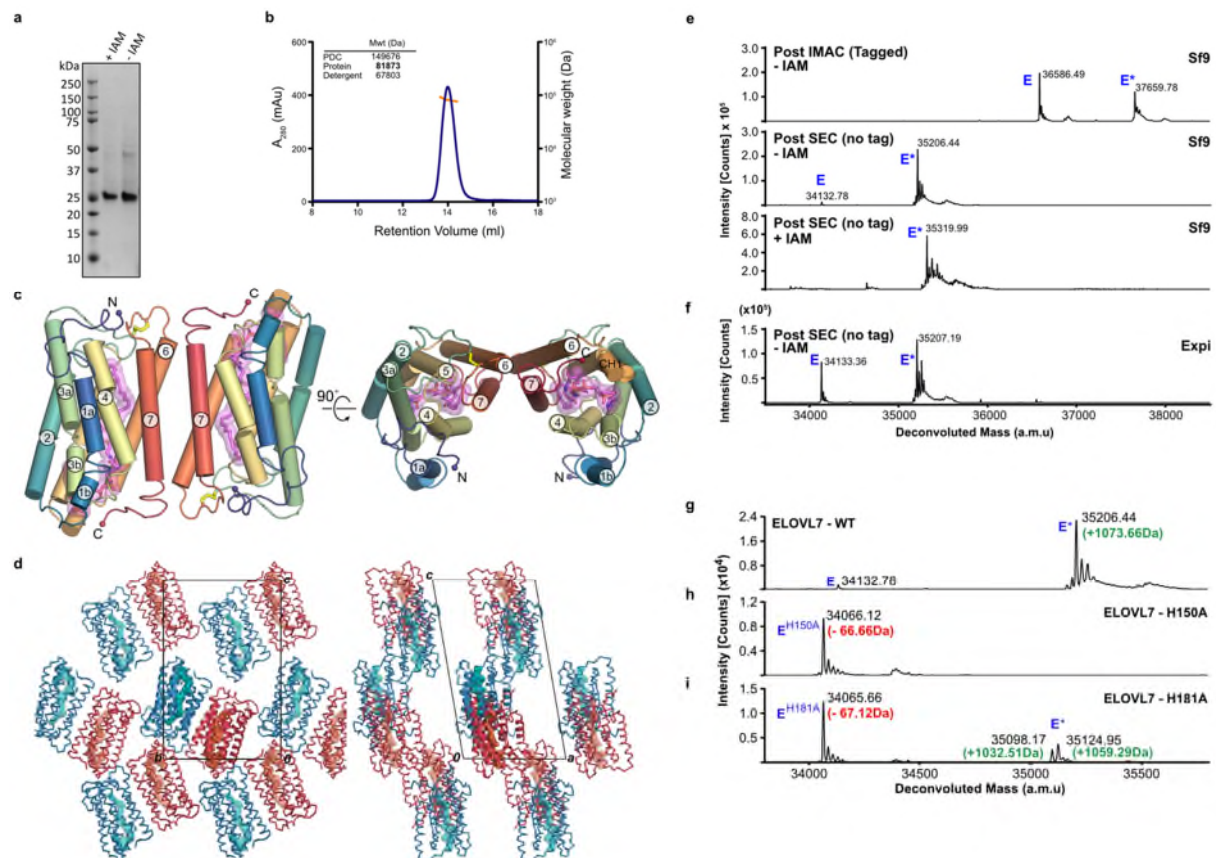


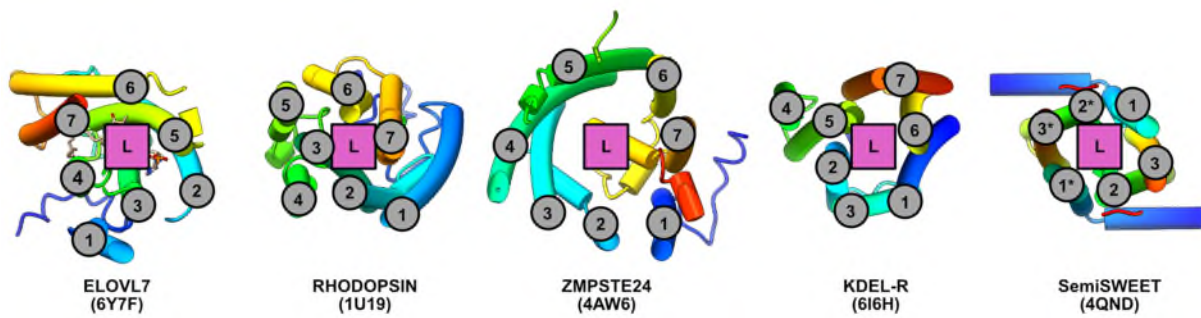
Extended Data Figures



Extended Data Fig. 1

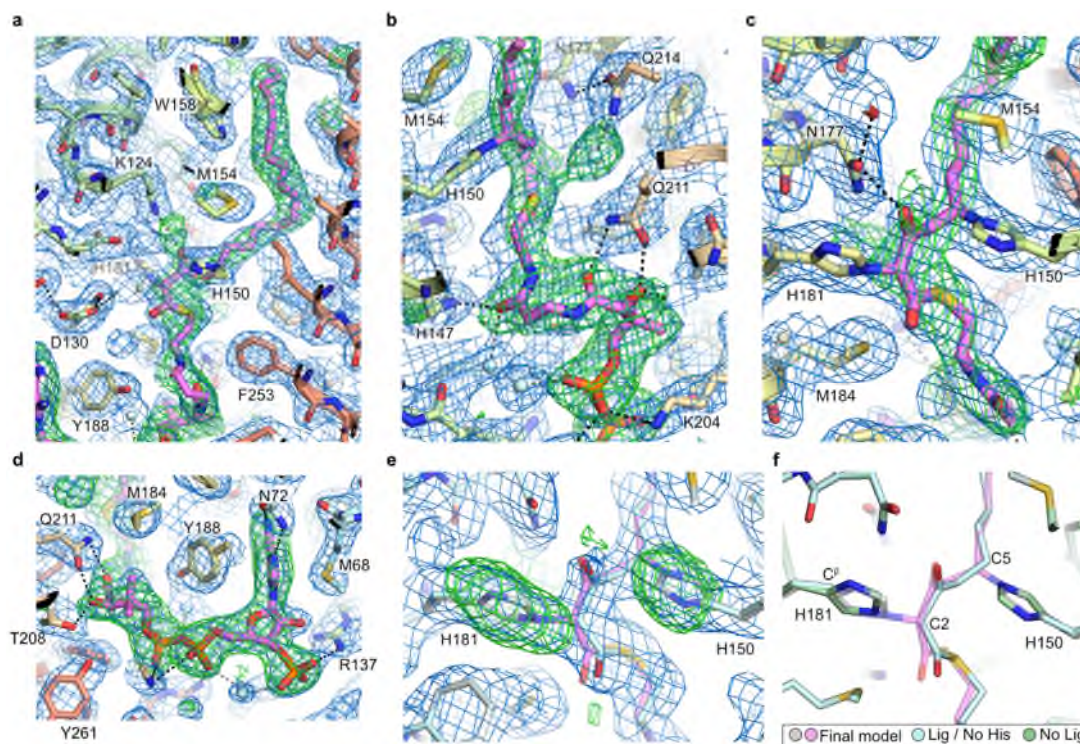
Properties of purified ELOVL7. **a**, SDS-PAGE gel of purified ELOVL7. Data shown is from a single purification but similar results were observed for multiple purifications / modifications. **b**, SEC profile and MALS analysis showing that OGNG-solubilised protein exists as a dimer in solution. Experiment carried out for tag-cleaved ELOVL7 purifications with and without IAM modification. Similar results were seen for each sample. **c**, Representation of head-to-tail dimer present in the crystal. **d**, ELOVL7 head-to-tail dimer packing within the crystal lattice. **e**, **f**, Intact mass analysis of ELOVL7 protein at various stages during purification. Deconvoluted mass spectra are shown for ELOVL7 protein purified from **(e)** *Sf9* ($n=3$ or 4) and **(f)** Expi293F cells ($n=2$). For protein purified after expression in insect cells, the samples are shown after immobilized metal affinity chromatography (IMAC), after cleavage of the tag and size exclusion chromatography (SEC) and after treatment with iodoacetamide (IAM). The expected mass of the untagged ‘native’ enzyme (E) based on the sequence is 34222.38 Da. The observed mass peaks (*Sf9*, 34132.78 Da; Expi 34133.36 Da) correspond to the loss of the N-terminal methionine (-131.20 Da) and acetylation of the resulting new N-terminus (+42.04 Da). All samples were run in their reduced state. The modified material (E*) appears as an adduct with an average mass shift of +1073.6 Da. The addition of 113.55 Da upon treatment with IAM suggests modification of two cysteine residues. **g-i**, Deconvoluted intact mass spectra for the untagged **g**, WT ($n=3$), **h**, H150A ($n=2$) and **i**, H181A mutants ($n=2$). The expected mass decrease of a His-to-Ala mutation is 66.06 Da. Evidence of *in vivo* modification (E*) is

observed for the H181A mutant but not for H150A. For intact mass experiments, theoretical and experimental masses along with mass errors are given in Supplementary Table 1.



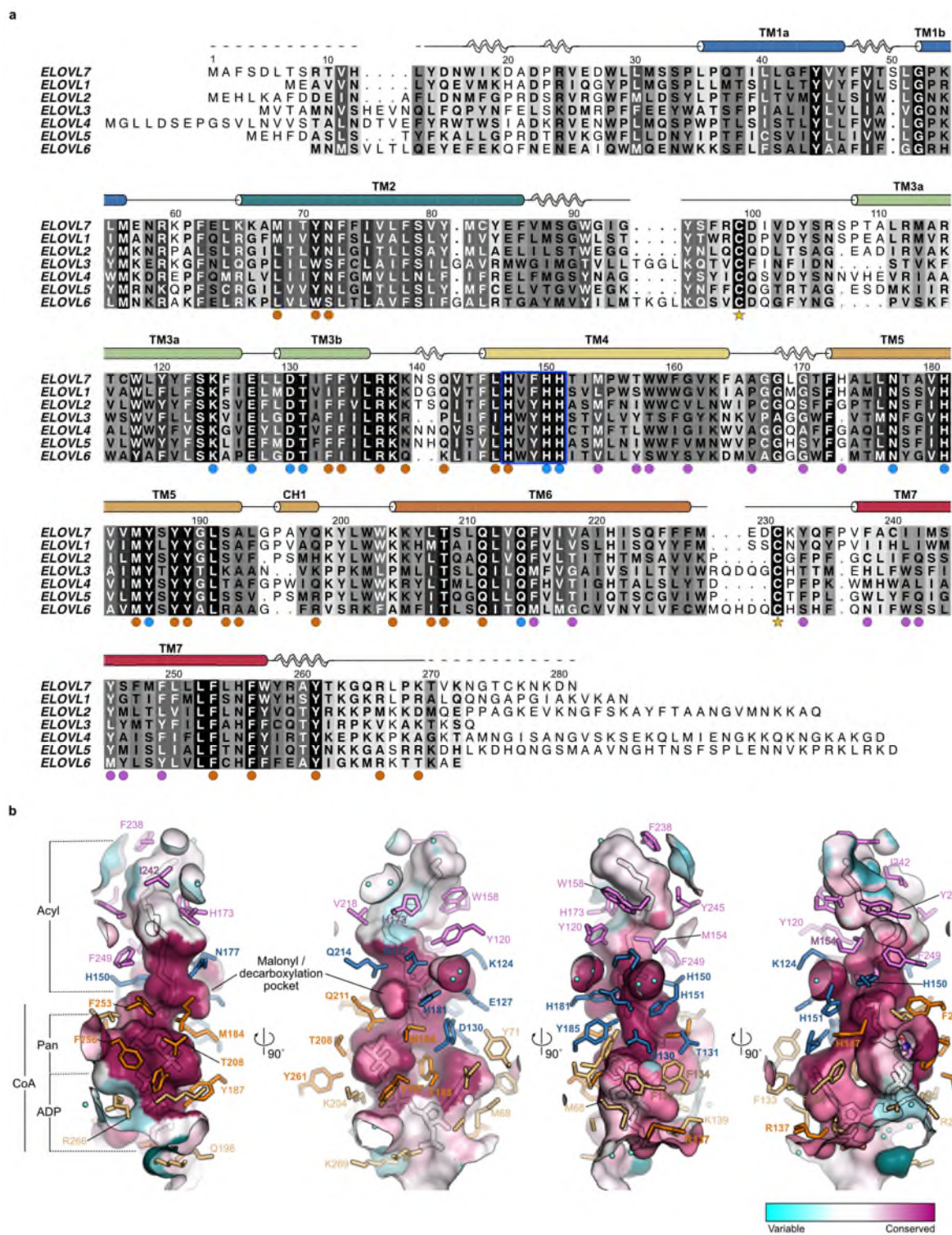
Extended Data Fig. 2

TM helix topology of ELOVL7. TM helical topology of ELOVL7 is compared with other six and seven membered TM bundles. TM helices are numbered and location of substrate/ligand site marked. Underlying cartoon representations of each structure are coloured from blue to red from the N- to C-termini respectively. PDB accession codes are shown in parentheses.



Extended Data Fig. 3

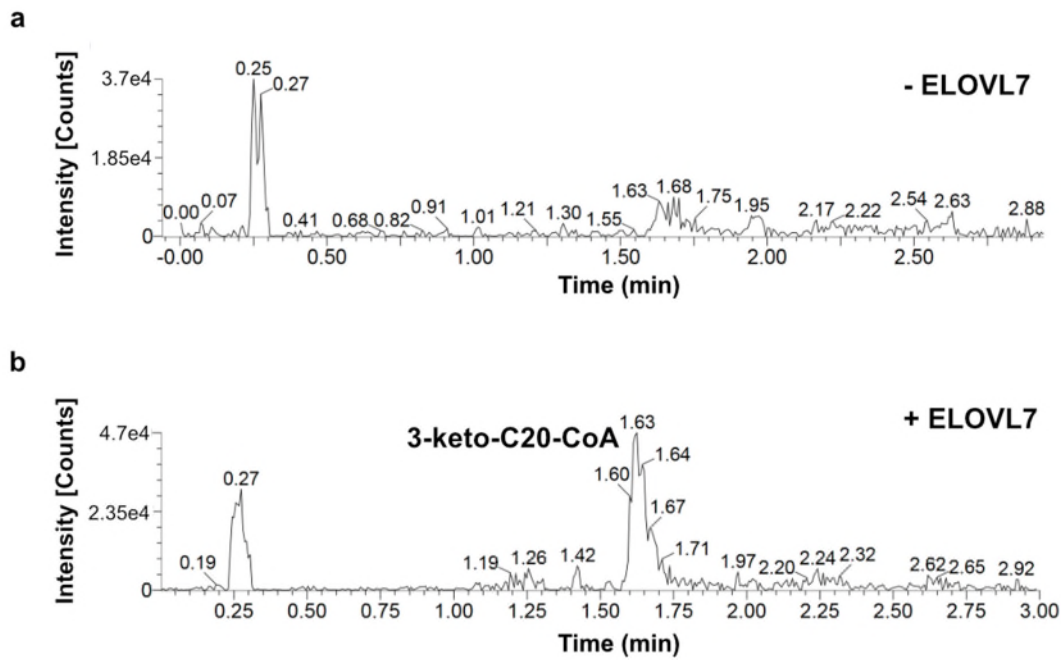
Electron density clearly shows covalently bound 3-keto-eicosanoyl-CoA. a-d, Electron density running along the catalytic tunnel. Final BUSTER 2mFo-DFc (blue mesh, contoured at 1σ) and omit mFo-DFc (green mesh, contoured at 2.5σ) electron density maps are overlaid on the final model. **e**, Comparison of a test refinement in which the imidazole groups of H150 and H181 were removed from the model (grey carbon protein atoms / palecyan ligand carbon atoms) and the final model (palecyan protein carbons / violet ligand carbon atoms). The BUSTER 2mFo-DFc (blue mesh, contoured at 1σ) and mFo-DFc (green mesh, contoured at 3σ) maps for the refined histidine-truncated model / unlinked acyl-CoA are shown. **f**, Comparison of various refined models (green carbons - protein only; palecyan - protein without H150/181 sidechain plus ligand; grey/violet - final model with covalently attached ligand).



Extended Data Fig. 4

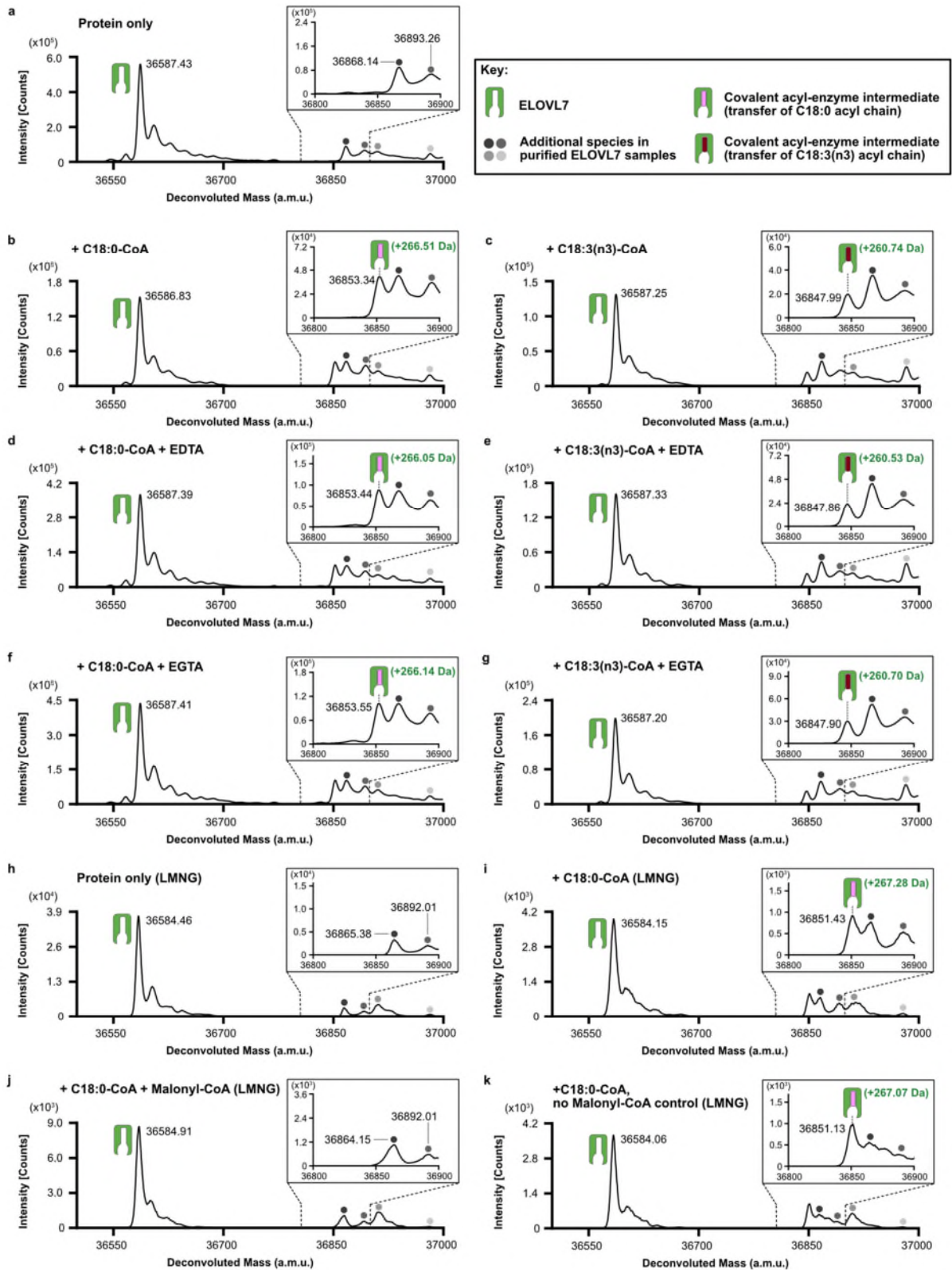
Sequence alignment and active site conservation of human ELOVL family members. a, Sequence alignment of human ELOVL1-7. The conserved histidine box ($^{147}\text{HxxHH}^{151}$) is highlighted by a blue box. Filled circles below alignment indicate residues with a proposed catalytic role (blue) and residues interacting with either the CoA (orange) or acyl (plum) portion of the substrate. Cysteines that form the disulphide bridge (C99-C231) between the TM2/3 and TM6/7 loops are indicated by stars. **b,** Conservation of active site tunnel. Molecular surface

representation is coloured by amino acid conservation score calculated by CONSURF analysis⁴⁹ of a diverse set of ELOVL1-7 family members. The various subregions of the tunnel are indicated (ADP / Pan from CoA and Acyl chain). Amino acid residues that form the binding tunnel are coloured according to region (pink, acyl; blue, catalytic site; orange CoA binding).



Extended Data Fig. 5

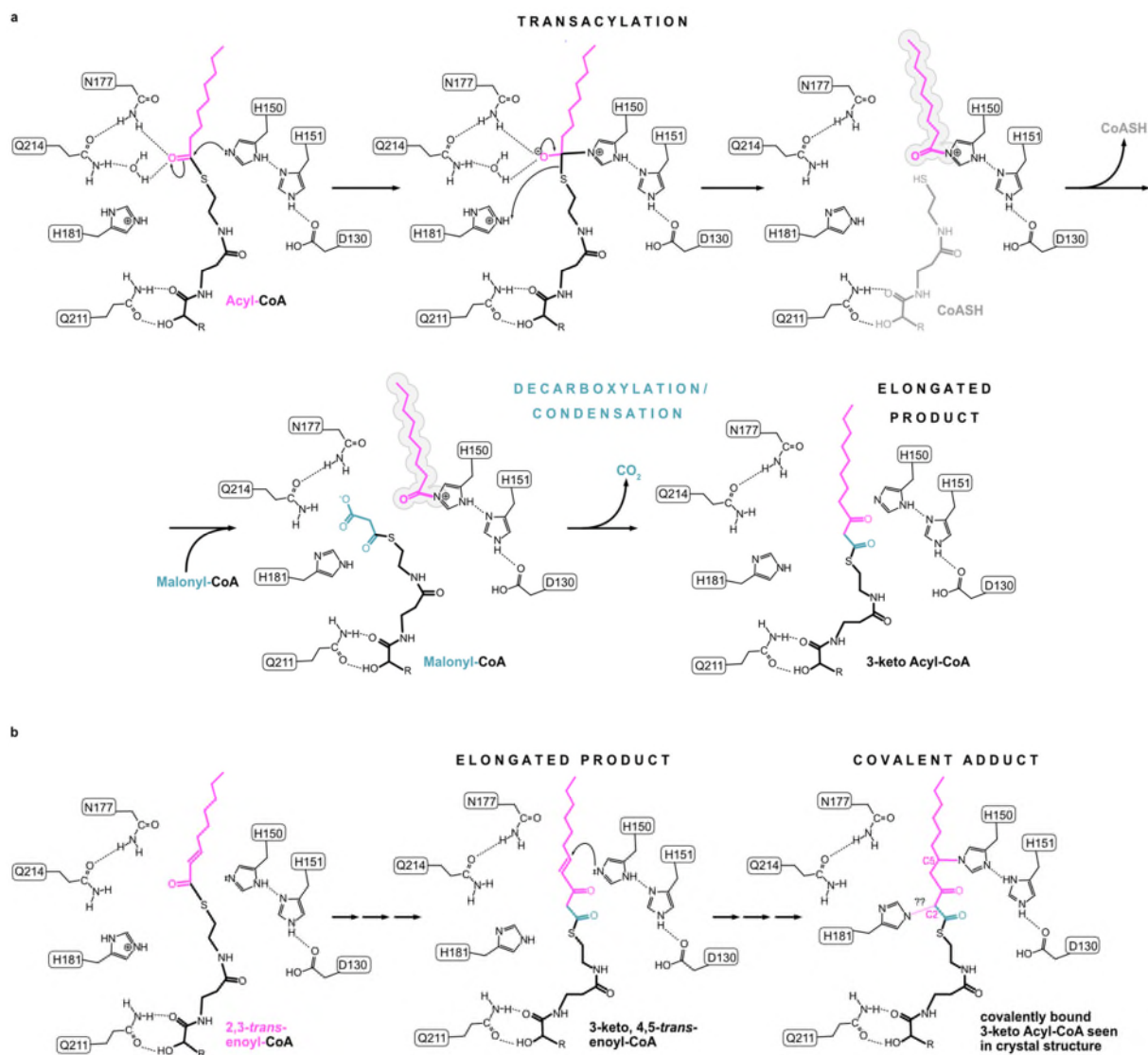
WT ELOVL7 activity. a,b Activity of residual WT enzyme on incubation with stearoyl-CoA (C18:0) and malonyl-CoA. Selected ion recording is shown for **a**, reaction mixture without added enzyme and **b**, reaction mixture after 3hr incubation with ELOVL7 enzyme. The ion peak at 1.61 mins corresponds to the expected 3-keto-eicosanoyl (C20)-CoA product of the elongation reaction. This experiment was carried out with two biological repeats with similar results.



Extended Data Fig. 6

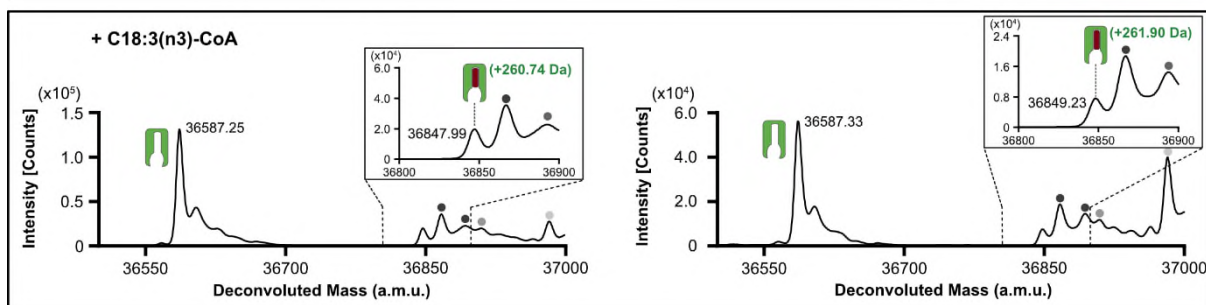
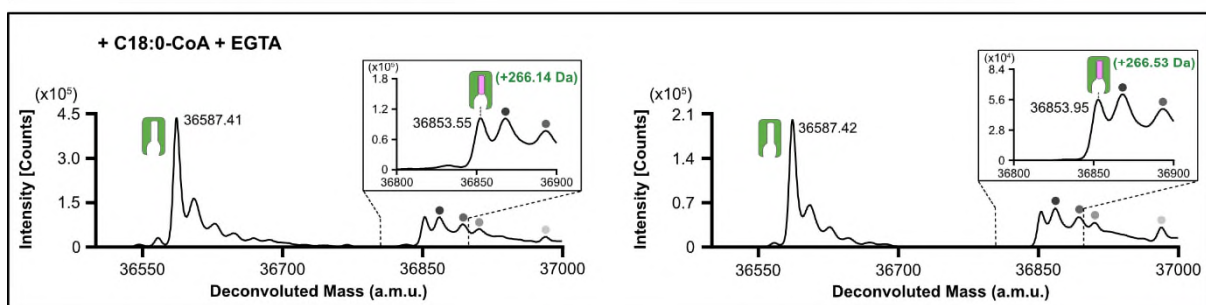
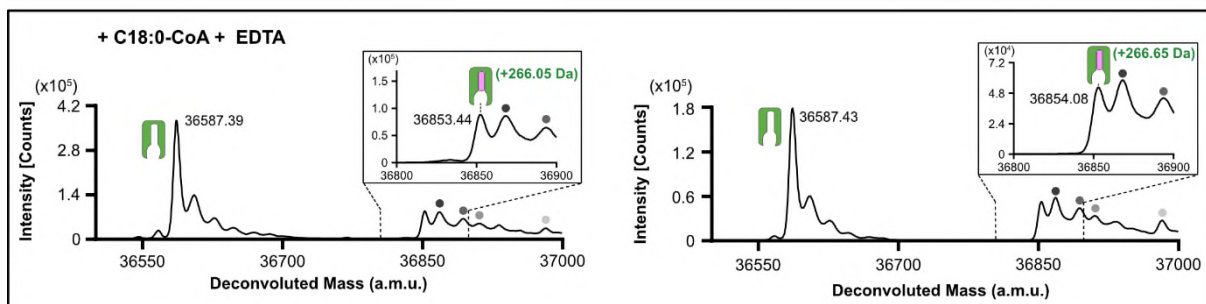
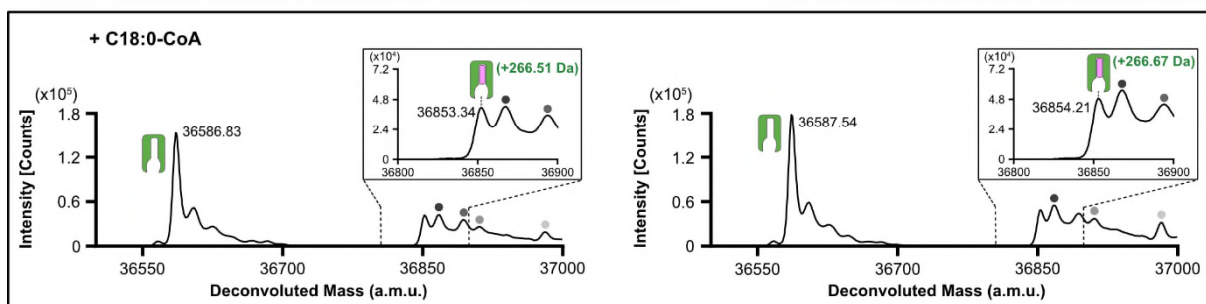
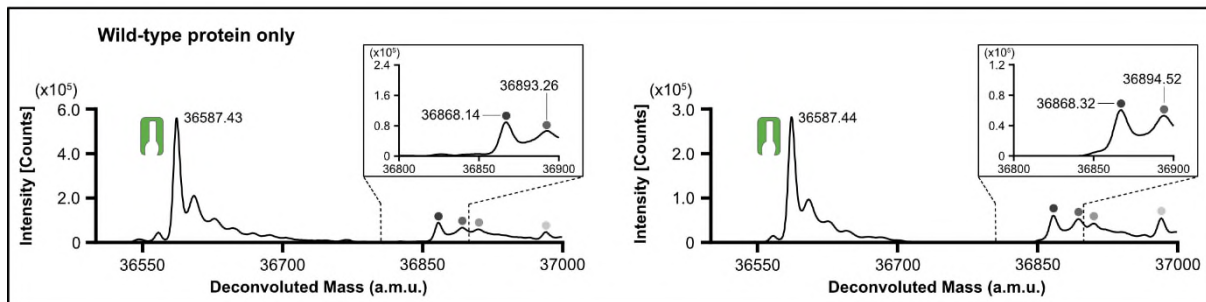
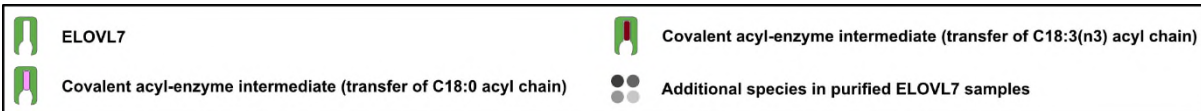
Identification of a covalent acyl-enzyme intermediate of ELOVL7. Purified, tagged, wild-type ELOVL7 was incubated in the presence and absence of known substrates and metal-chelating agents prior to LC-ESI-MS intact mass analysis. **a-g**, Deconvoluted intact mass spectra for ELOVL7 incubated for 2h at 37°C. **a**, in the absence of substrates. **b**, ELOVL7

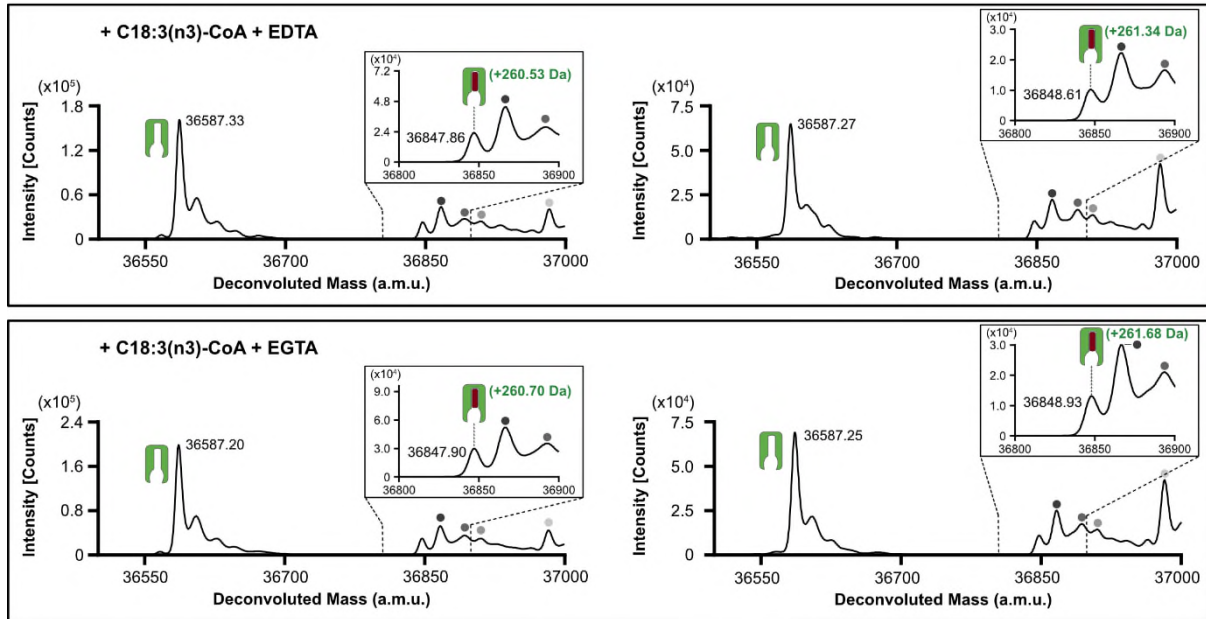
incubated with 100 μ M C18:0-CoA. Expected mass addition for acyl intermediate upon reaction with C18:0-CoA: +266.47 Da. **c**, ELOVL7 incubated with 100 μ M C18:3(n3)-CoA. Expected mass addition for acyl intermediate upon reaction with C18:3(n3)-CoA: +260.42 Da. **d-e**, ELOVL7 incubated with **d**, 100 μ M C18:0-CoA or **e**, 100 μ M C18:3(n3)-CoA in the presence of 1mM EDTA. **f-g** ELOVL7 incubated with **f**, 100 μ M C18:0-CoA or **g**, 100 μ M C18:3(n3)-CoA in the presence of 1mM EGTA. **h-k**, Sequential reaction of LMNG-purified ELOVL7 with C18:0-CoA and malonyl-CoA. **h**, LMNG-purified ELOVL in the absence of substrates. **i**, ELOVL7 incubated with 100 μ M C18:0-CoA. **j**, Purified ELOVL7 initially incubated with 100 μ M C18:0-CoA, followed by incubation with 200 μ M malonyl-CoA. Addition of the second substrate leads to loss of the acyl-enzyme intermediate peak, consistent with the reaction having gone to completion. **k**, control ELOVL7 sample taken after incubation with C18:0-CoA was further incubated in the absence of malonyl-CoA, showing that covalent intermediate loss only occurs in the presence of malonyl-CoA. All experiments were repeated independently twice with similar results (n=2 biological repeats, see Supplementary Figure 1 and Figure 2 for replicate traces. See Supplementary Table 2 for theoretical and experimental masses and mass errors).



Extended Data Fig. 7

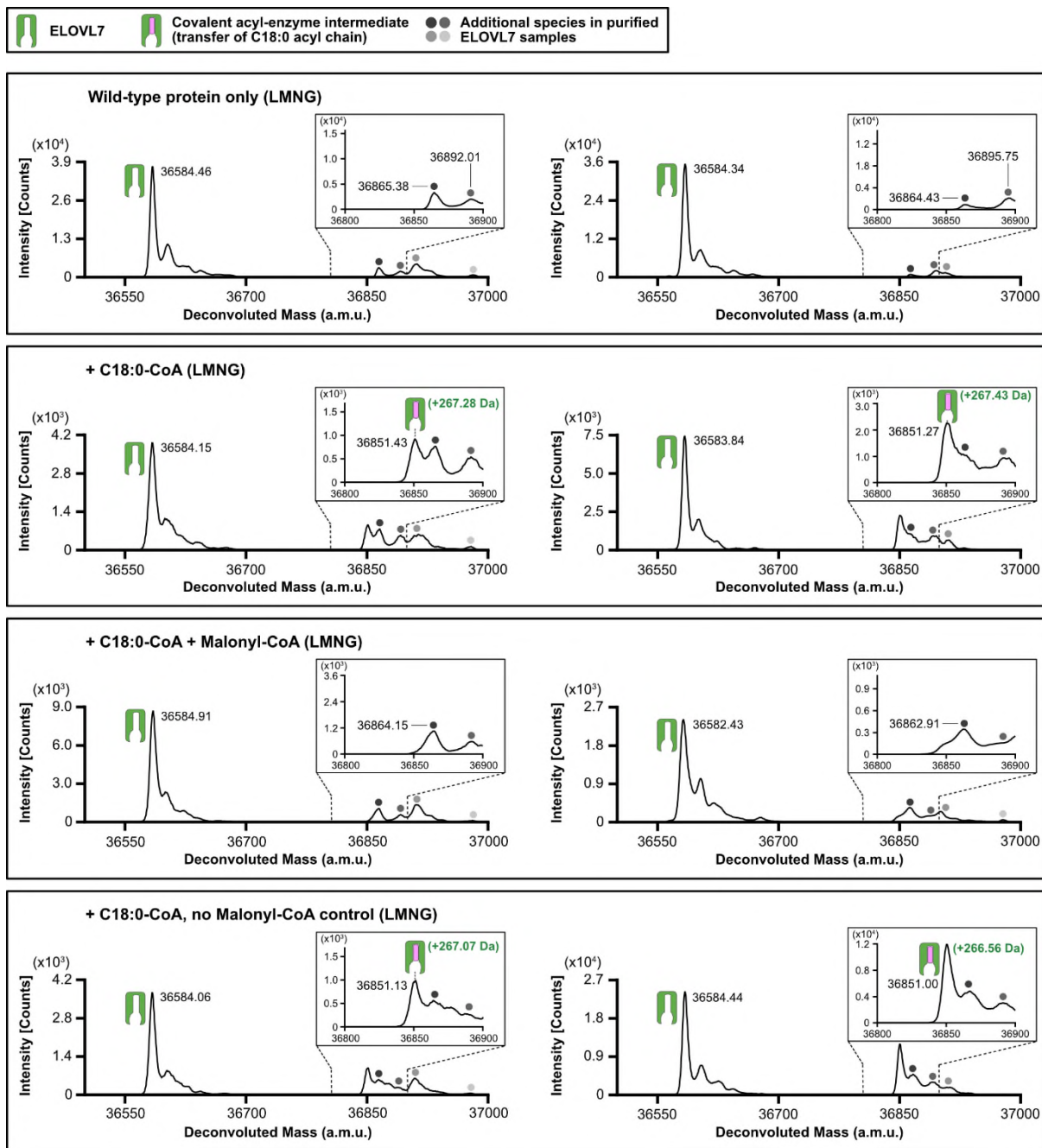
Proposed ping-pong reaction mechanism for ELOVL7. **a**, Transacylation step with acyl chain of first substrate being transferred to H150. In the second step, malonyl-CoA binds and undergoes decarboxylation and a condensation reaction to form the elongated 3-keto product. **b**, Proposed reaction steps leading to C-N covalent adduct with H150 seen in crystal structure. In this scenario a 2,3-*trans*-enoyl-CoA serves as the first substrate (*left*) leading to the 3-keto,4,5-*trans*-enoyl-CoA ‘product’ (*middle*) which subsequently crosslinks to H150 via a conjugate addition reaction of H150 (*right*). The nature of the reaction that leads to H181 crosslinking to the C2 atom of the 3-keto-acyl-CoA is not clear.





Supplementary Fig. 1 Identification of a covalent acyl-enzyme intermediate of ELOVL7

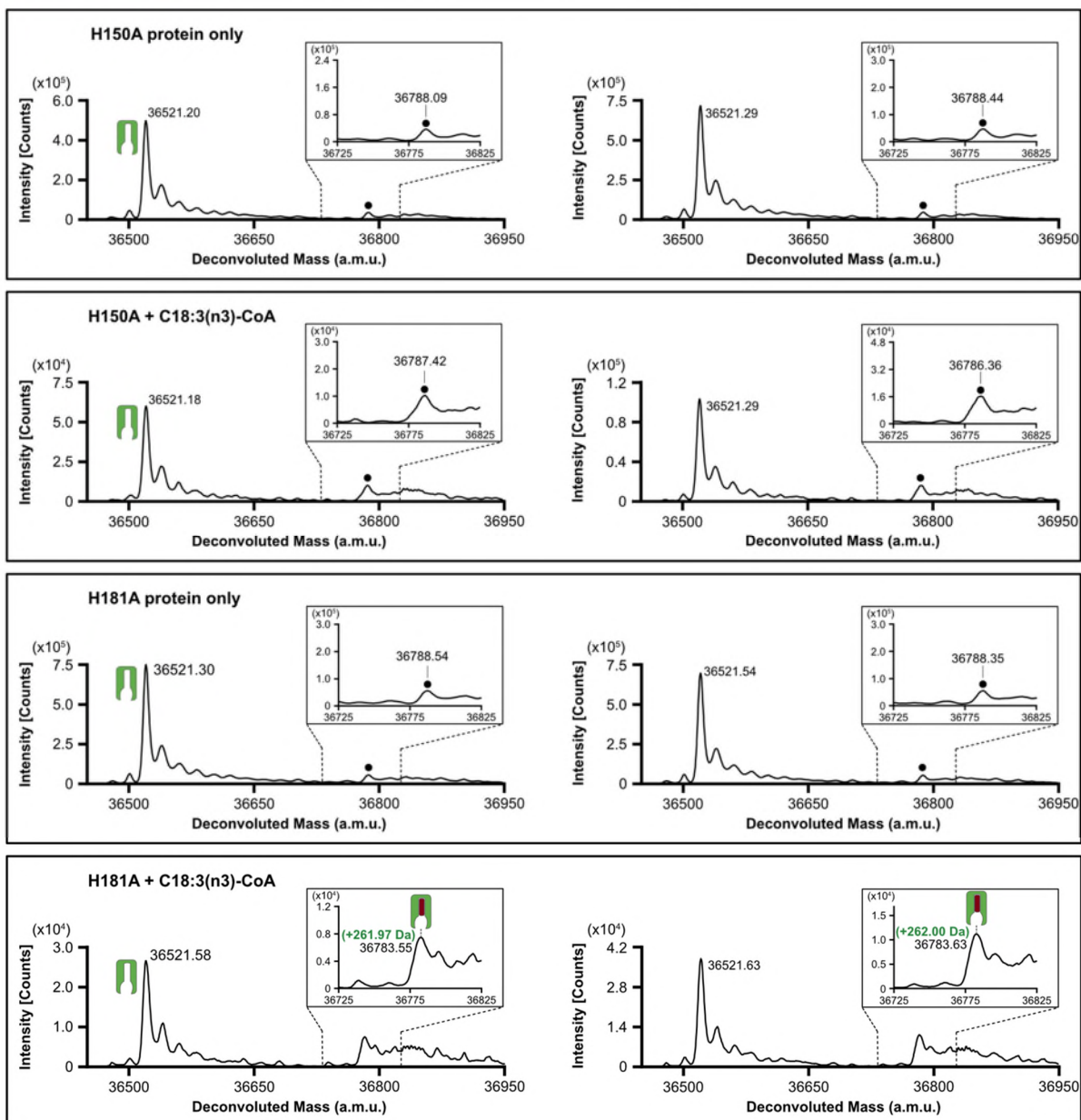
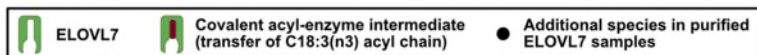
Replicate intact mass spectrometry data for experiments presented in Extended Data Figure 6. Purified, tagged, wild-type ELOVL7 was incubated for 2h at 37°C in the presence and absence of known substrates and metal-chelating agents prior to LC-ESI-MS intact mass analysis. Deconvoluted intact mass spectra are shown side-by-side for two independent experiments. Spectra are shown for ELOVL7 incubated in the absence of substrates, with 100µM C18:0-CoA (expected mass addition for acyl intermediate upon reaction with C18:0-CoA: +266.47 Da), with 100µM C18:0-CoA in the presence of either 1mM EDTA or 1mM EGTA. Identical experiments were performed with a different acyl-CoA substrate (100µM C18:3(n3)-CoA). Expected mass addition for acyl intermediate upon reaction with C18:3(n3)-CoA: +260.42 Da. The inset panel is a zoomed view of the region that encompasses the mass range where the acyl covalent intermediate would be present.



Supplementary Fig. 2. Sequential reaction of LMNG-purified ELOVL7 with C18:0-CoA and malonyl-CoA

Replicate intact mass spectrometry data for experiments presented in Extended Data Figure 6. Purified, tagged, ELOVL7 in LMNG was initially incubated for 15 mins at 37°C with 100µM C18:0-CoA. At the end of this incubation, any precipitated protein was removed by centrifugation and the soluble fraction was analysed by LC-ESI-MS. Then, 200µM malonyl-CoA was added and the mixture was incubated for 3h at 4°C. Incubation with malonyl-CoA led

to the loss of the covalent intermediate deconvoluted mass peak, consistent with the reaction having gone to completion. Control samples taken after incubation with C18:0-CoA were also incubated for 3h at 4° C in the absence of malonyl-CoA. Deconvoluted intact mass spectra are shown side-by-side for two independent experiments. The inset panel is a zoomed view of the region that encompasses the mass range where the acyl covalent intermediate would be present. Expected mass shift upon reaction with C18:0 CoA: +266.47 Da.



Supplementary Fig. 3 Covalent acyl-enzyme intermediate is formed upon substrate reaction at H150.

Replicate intact mass data for experiments presented in Figure 6. LC-ESI-MS intact mass analysis of H150A and H181A mutant proteins are shown after incubation with either no substrate or an acyl-CoA (100 μ M C18:3(n3)-CoA) at 37 $^{\circ}$ C for 2h. Deconvoluted intact mass spectra are shown side-by-side for two independent experiments. The inset panel is a zoomed

view of the region that encompasses the mass range where the acyl covalent intermediate would be present. Expected mass shift upon reaction with C18:3(n3)-CoA: +260.42 Da.

Supplementary Table 1: Theoretical and experimental deconvoluted masses from denaturing intact mass spectrometry experiments shown in Fig. 2c and Extended Data Figure 1.

Sample	Unmodified protein			3-keto eicosanoyl(C20)-CoA adduct		
	Theoretical ^a (a.m.u)	Experimental (a.m.u)	Mass error (ppm)	Theoretical ^b (a.m.u)	Experimental (a.m.u)	Mass error (ppm)
WT Post IMAC – IAM (<i>Sf9</i>) (EDF1e)	36586.67	36586.49	-5	37660.69	37659.78	-24
WT Post SEC –IAM (<i>Sf9</i>) (Fig. 2c, EDF1e,g)	34133.22	34132.78	-13	35207.24	35206.44	-23
WT Post SEC +IAM (<i>Sf9</i>) (EDF1e)	34247.36 ^c	No peak observed	-	35321.38 ^c	35319.99	-39
WT Post SEC –IAM (Expi) (EDF1f)	34133.22	34133.36	4	35207.24	35207.19	-1
H150A Post SEC – IAM (<i>Sf9</i>) (EDF1h)	34067.15	34066.12	-30	35141.17	No peak observed	-
H181A Post SEC – IAM (<i>Sf9</i>) (EDF1i)	34067.15	34065.66	-44	35141.17	No peak observed	-

^a Theoretical masses shown for unmodified protein correspond to the predicted mass of purified, tagged (post IMAC) or untagged (post SEC), ELOVL7 protein (wild-type, H150A and H181A mutants) with loss of the initiator methionine and acetylation of the new N-terminus.

^b Theoretical masses of 3-keto eicosanoyl(C20)-CoA adducts correspond to a mass shift of +1074.02 Da.

^c Theoretical masses of +IAM samples include a +114.14 Da mass shift corresponding to IAM modification at 2 sites.

Supplementary Table 2: Theoretical and experimental deconvoluted masses from covalent intermediate formation denaturing intact mass spectrometry experiments.

Sample	Unmodified protein			Acyl-enzyme intermediate		
	Theoretical ^a (a.m.u)	Experimental (a.m.u)	Mass error (ppm)	Theoretical ^b (a.m.u)	Experimental (a.m.u)	Mass error (ppm)
WT protein only (Fig. 5b, EDF 6a)	36586.67	36587.43	21	-	-	-
WT protein only (Replicate #2)	36586.67	36587.44	21	-	-	-
WT + C18:0-CoA (Fig. 5b, EDF 6b)	36586.67	36586.83	4	36853.14	36853.34	5
WT + C18:0-CoA (Replicate #2)	36586.67	36587.54	24	36853.14	36854.21	29
WT + C18:3(n3)-CoA (Fig. 5b, EDF 6c)	36586.67	36587.25	16	36847.09	36847.99	24
WT + C18:3(n3)-CoA (Replicate #2)	36586.67	36587.33	18	36847.09	36849.23	58
WT + C18:0-CoA + EDTA (EDF 6d)	36586.67	36587.39	20	36853.14	36853.44	8
WT + C18:0-CoA + EDTA (Replicate #2)	36586.67	36587.43	21	36853.14	36854.08	26
WT + C18:3(n3)-CoA + EDTA (EDF 6e)	36586.67	36587.33	18	36847.09	36847.86	21
WT + C18:3(n3)-CoA + EDTA (Replicate #2)	36586.67	36587.27	16	36847.09	36848.61	41
WT + C18:0-CoA + EGTA (EDF 6f)	36586.67	36587.41	20	36853.14	36853.55	11
WT + C18:0-CoA + EGTA (Replicate #2)	36586.67	36587.42	20	36853.14	36853.95	22
WT + C18:3(n3)-CoA + EGTA (EDF 6g)	36586.67	36587.20	14	36847.09	36847.90	22
WT + C18:3(n3)-CoA + EGTA (Replicate #2)	36586.67	36587.25	16	36847.09	36848.93	50
WT protein only (LMNG) (Fig. 5c, EDF 6h)	36586.67	36584.46	-60	-	-	-
WT protein only (LMNG) (Replicate #2)	36586.67	36584.34	-64	-	-	-
WT + C18:0-CoA (LMNG) (Fig. 5c, EDF 6i)	36586.67	36584.15	-69	36853.14	36851.43	-46
WT + C18:0-CoA (LMNG) (Replicate #2)	36586.67	36583.84	-77	36853.14	36851.27	-51
WT + C18:0-CoA + Malonyl-CoA (LMNG) (Fig. 5c, EDF 6j)	36586.67	36584.91	-48	36853.14	No peak observed	-
WT + C18:0-CoA + Malonyl-CoA (LMNG) (Replicate #2)	36586.67	36582.43	-116	36853.14	No peak observed	-
WT + C18:0-CoA control (LMNG) (EDF 6k)	36586.67	36584.06	-71	36853.14	36851.13	-55
WT + C18:0-CoA control (LMNG) (Replicate #2)	36586.67	36584.44	-61	36853.14	36851.00	-58
H150A protein only (Fig. 6b)	36520.61	36521.20	16	-	-	-
H150A protein only (Replicate #2)	36520.61	36521.29	19	-	-	-
H150A + C18:3(n3)-CoA (Fig. 6b)	36520.61	36521.18	16	36781.03	No peak observed	-
H150A + C18:3(n3)-CoA (Replicate #2)	36520.61	36521.29	19	36781.03	No peak observed	-
H181A protein only (Fig. 6c)	36520.61	36521.30	19	-	-	-
H181A protein only (Replicate #2)	36520.61	36521.54	25	-	-	-
H181A + C18:3(n3)-CoA (Fig. 6c)	36520.61	36521.58	27	36781.03	36783.55	69
H181A + C18:3(n3)-CoA (Replicate #2)	36520.61	36521.63	28	36781.03	36783.63	71

^a Theoretical masses shown for unmodified protein correspond to the predicted mass of purified, tagged ELOVL7 protein –IAM (wild-type, H150A and H181A mutants) with loss of the initiator methionine and acetylation of the new N-terminus.

^b Theoretical masses of acyl-enzyme intermediates correspond to a mass shift of +266.47 Da upon reaction with C18:0-CoA or +260.42 Da upon reaction with C18:3(n3)-CoA.